ELSEVIER

Cement & Concrete Composites 25 (2003) 557–564

Cement & Concrete Composites

www.elsevier.com/locate/cemconcomp

Aggregate/mortar interface: influence of silica fume at the micro- and macro-level

Sinan Caliskan *

Department of Civil Engineering, School of Engineering, University of Dundee, Dundee DD1 4HN, UK

Abstract

Microstructural investigations and chemical analyses were conducted by utilizing scanning electron microscopy and energy dispersive X-ray analyser in the interfacial zone between three types of cylindrical aggregates (sandstone, limestone and granite) and two types of mortar matrices (plain mortar and 20% silica fume mortar). The strength of the interface was determined experimentally by means of aggregate push-out test. Interfacial strength was then related to the interfacial thickness and the amount of silica at the interface. It was found that the higher the silica concentration in the interface, the thinner the relative interfacial thickness and the higher the interfacial bond strength as a result of the densification role of silica fume. The interfacial bond strength was found to increase as the aggregate size decreased, irrespective of the type of aggregate and the mortar matrix. This size effect is shown to be statistical in nature and described by Weibull theory.
© 2002 Elsevier Science Ltd. All rights reserved.

Keywords: Interface; Silica fume; Interfacial bond strength; Size effect; Scanning electron microscopy; Chemical analysis

1. Introduction

Concrete is generally referred to as a heterogeneous and discontinuous material and is formed primarily by mixing three constituents, namely aggregate, cement and water. Coarse and fine aggregates are bound together by the adhesive character of cement paste into a rock-like mass, concrete. Due to the different phases that interact with each other during the formation stage, the heterogeneous nature of concrete is unavoidable. As a result, concrete suffers from microcracks and flaws including pores, air voids, lenses of bleed water and shrinkage cracks even in the unloaded stage. When external loading is applied, these microcracks grow and coalesce with new microcracks leading to the failure of the structure or member [1,2].

The overall quality of concrete is usually evaluated by means of its strength, which is directly dependent upon the microstructure. The strength of concrete is a vital requirement for structural design and is specified for compliance purposes. However, other characteristics of concrete, such as durability and permeability, may be more important in some practical cases [3]. As concrete finds usage in new and varied applications, understanding the microstructure particularly at the aggregate–matrix interface, and the influence this has upon concrete properties, becomes more critical. In particular, the increased demand to obtain high performance cementitious composite materials, including strength, ductility and durability, in recent years has resulted in renewed interest in the study of the interfaces between the constituents [4–9].

It is generally accepted that a weak interfacial zone exists between aggregates and matrix in all cement based materials. Cracks in concrete propagate preferentially along this weak zone. Over the years, this zone has been analysed from different aspects and it has been concluded that its properties have a significant influence on the short term and long-term behaviour and performance of concrete materials [4,10–14]. A weak interfacial zone may have many serious influences on a range of properties of concrete, e.g. concrete in a severe marine environment. Water and harmful ions will easily penetrate into the concrete resulting in the deterioration of both the concrete and the reinforcement. Therefore, it is essential for the long-term performance of concrete that the interfacial zone should be as dense as possible, having a strong bond between the aggregate and the cement matrix [15].

* Tel.: +44-1382-344874; fax: +44-1382-344816.
E-mail address: s.caliskan@dundee.ac.uk (S. Caliskan).

0958-9465/03/$ - see front matter © 2002 Elsevier Science Ltd. All rights reserved.
doi:10.1016/S0958-9465(02)00095-1

Despite the significance of the interfacial zone on the overall short and long-term performance of cement based composite materials, the nature of the interface and the interfacial bond is not fully understood. Moreover, the determination of the quality of the bond between aggregate and the matrix is rather difficult and no standardised test method is available. There is a need, therefore, to undertake research that aims to explore the properties and the behaviour of the interfacial zone between aggregate particles and matrices in concrete.

2. Experimental details

2.1. Materials

The test specimens used in the microstructural study and the aggregate push-out experiments are composed mainly of two parts: the mortar matrix and the cylindrical aggregate. Fig. 1 shows the details of the specimen. The matrix part was formed by two types of mortar (plain and 20% SF cement) composed of Ordinary Portland cement (Table 1), locally supplied sea-dredged fine aggregate (particle size range between 212 and 5000 μm), water and where applicable 20% silica fume in powder form (Elkem Microsilica) and superplasticiser (SP) (Conplast SP430), while the cylindrical aggregates shown in Fig. 2 were three types (sandstone, limestone and granite) with four different diameters (10, 14, 20 and 30 mm). Table 1 shows chemical analysis of cement. The mix proportions and the mechanical properties (obtained by using the relevant test methods described by the British Standard Institution, namely compressive strength [16], tensile strength [17] and modulus of elasticity [18]) of the mortar matrix are given in Tables 2 and 3, respectively, while the compressive strength results (obtained by using the test method described in reference [19]) of aggregate types are given in Table 4.

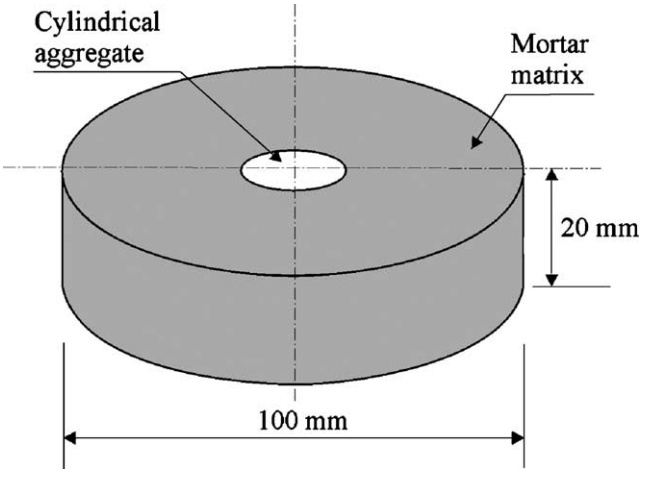

Fig. 1. Schematic view of a push-out test specimen.

Table 1
Chemical analysis of Portland cement sample used in the mortar

Oxides	
SiO_2	19.4%
Al_2O_3	4.2%
Fe_2O_3	2.1%
CaO	63.4%
MgO	2.4%
SO_3	3.1%
K_2O	0.62%
Na_2O	0.16%
Loss on ignition	3.4%
Free lime	1.4%
Compounds	
C_3S	62.8%
C_2S	8.9%
C_3A	7.5%
C_4AF	6.4%
Eq. Na_2O	0.57%

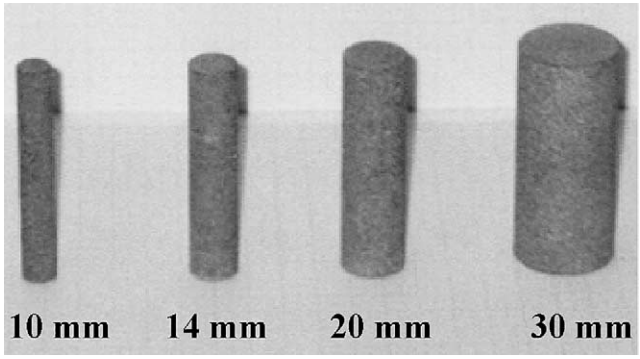

Fig. 2. Four different diameters of cylindrical aggregates.

2.2. Preparation of specimens

Initially, the cylindrical aggregates were cored from mother rocks and cut to a length of 45, 25 mm of which was located into the central hole of the cylindrical disc at the bottom of the 100 mm diameter steel mould to maintain its precise vertical position during casting. The cylindrical aggregates were kept in a water tank for 24 h before casting to maintain constant surface wetness. Prior to casting, they were taken out and any excessive water on the surfaces was dried by a cloth. After applying a thin layer of lubricant to the mould and locating the aggregate in the center, the gap between the aggregate and the inner surface of the mould was filled with mortar on a vibrating table. After 28 days of standard water curing at a temperature of 20 °C, the samples were ready to be used in both aggregate push-out tests and thin section preparation for microstructural investigations.

Table 2
Mix proportions of mortars

Mortar type	C	S	W/B	W/C	SF % C	SP (ml/kg of B)	B (kg/m^3)	C (kg/m^3)
Plain	1	2.5	0.5	0.5	–	–	612.5	612.5
20% SF	1	2.5	0.3	0.38	20	35	645	515

C: cement, S: sand, W/B: water to binder ratio, W/C: water to cement ratio, B: binder, SF: silica fume, SP: superplasticiser.

Table 3
Mechanical properties of mortar matrices (with coefficients of variation as (%))

Mortar type	Nominal compressive strength (MPa)	Actual compressive strength (MPa)	Tensile strength (MPa)	Elastic modulus (GPa)
Plain	40	38.6 (3.79)	3.0 (4.30)	27.5
20% SF	80	78.1 (7.32)	4.3 (9.68)	36.2

Table 4
Compressive strength of sandstone, limestone and granite rocks (with coefficients of variation (%))

Aggregate	Nominal compressive strength (MPa)	Actual compressive strength (MPa)
Sandstone	100	102.8 (3.39)
Limestone	150	147.3 (32.77)
Granite	180	179.1 (43.45)

The test specimens containing the 10 mm diameter cylindrical aggregates in the center were selected to be used in the microstructural investigations. With the use of only 10 mm diameter, it was possible to include the aggregate and the surrounding mortar matrix within the 25 mm width of thin section glass slide. Therefore, for all combinations of aggregate and mortar types, a total of 12 thin sections were prepared, six of which contained the aggregates in horizontal position shown in Fig. 3 and the other six thin sections contained the same type of aggregate in the vertical position as shown in Fig. 4. Hence, from the same test specimen, two thin sections were prepared. This was done by first splitting the test specimen horizontally in two halves of about 10 mm thicknesses. Then, one part was used for the thin section containing the aggregate in the horizontal position and the other half was used for the thin section containing the aggregate in the vertical position. By preparing two thin sections from the same test specimen in different directions, larger interfacial area was analyzed. The Logitech Precision Lapping machine was used with 600 grit silicon carbide to grind the 10 mm thickness down to a few mm thick specimen that was then glued on to a glass plate with resin. They were again lapped to obtain a thickness of approximately 30 μm. The thickness of the scanning electron microscopy (SEM) samples is dictated by the time required for the evacuation of the chamber.

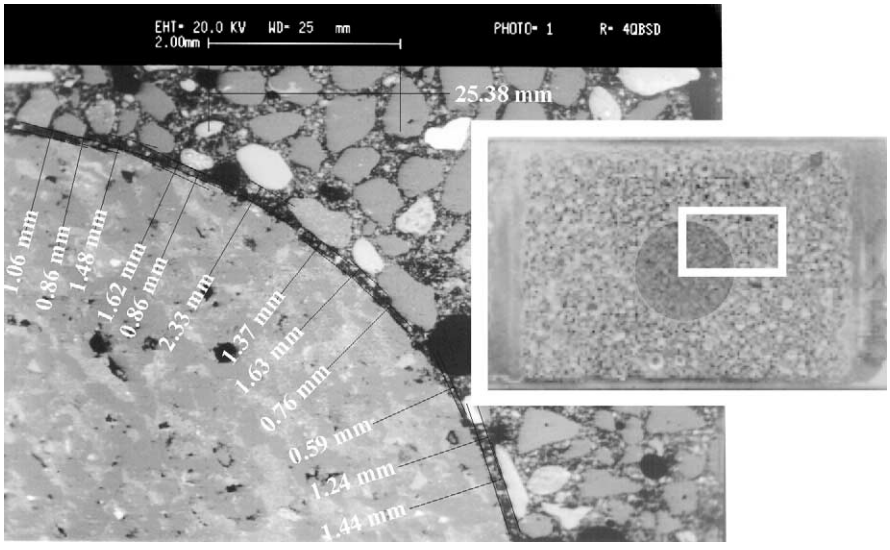

Fig. 3. A horizontal thin section and a SEM image showing the relative interfacial thickness reading pattern.

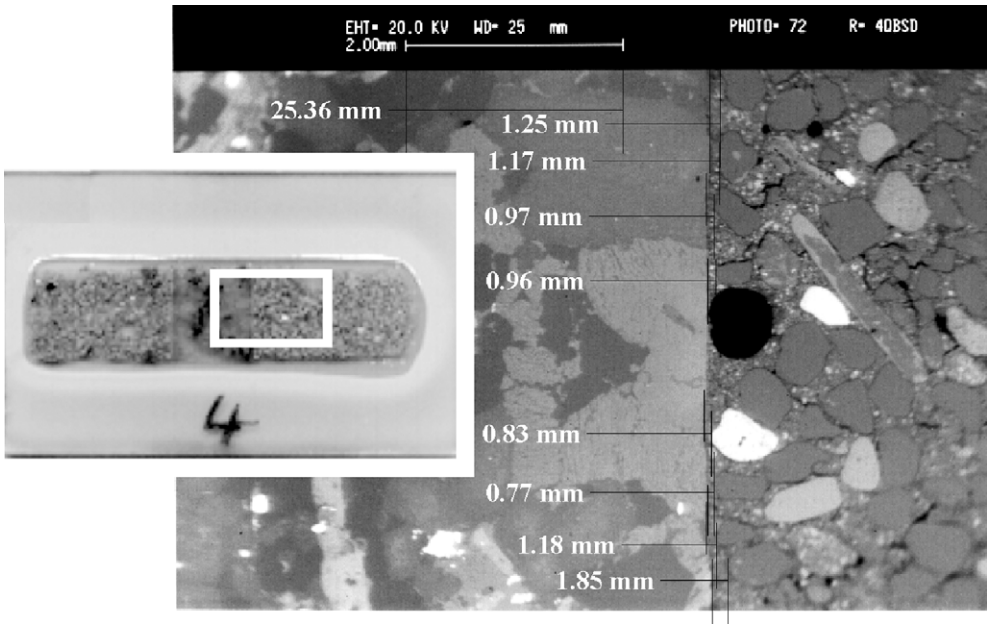

Fig. 4. A vertical thin section and a SEM image showing the relative interfacial thickness reading pattern.

The thin sections could now be polished. The Struers-DAP-2 polishing machine was employed to polish the thin sections with 0.3 μm aluminium oxide grit, which gives satisfactory results and good finish when mixed with distilled water (mix proportion was 1:1). When the polishing was completed, the surfaces of the sections were cleaned by compressed air and left to dry for a day. Thin sections were carbon coated prior to the SEM investigation. The prescribed lapping process only removes the surface layer disturbed by sawing but does not introduce cracks into the specimen.

2.3. Experimental method for microstructural study

The interface does not present distinctly defined borders, so the zone between the cylindrical aggregate and the mortar matrix, which is clearly free of sand particles, is assumed to be the interfacial zone. This zone is essentially filled by primary and where applicable (when SF is used) secondary hydration products. As this study is mainly concerned with the comparison of different types of aggregate and different types of mortar, a relative thickness of the interface between two different phases (aggregate/mortar) is adequate and absolute value of thickness is not required.

For each small interfacial thickness reading between the sand particles and cylindrical aggregate, the area on the SEM images was digitally magnified approximately 5000-fold. Average of 10 readings, as shown in Figs. 3 and 4, were taken on each thin section. The interfacial zone thickness of an aggregate type was then obtained by the average of the readings of the horizontal and vertical thin sections.

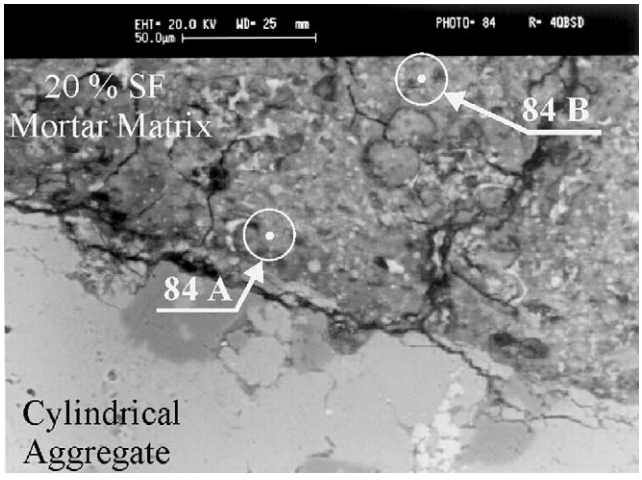

Fig. 5. SEM image showing the points selected in the interface for chemical analysis.

By energy dispersive X-ray (EDX) analyser, chemical analyses of interfacial zone were conducted, an example of which is given in Fig. 5. For this purpose, average of three points were defined in the interfacial zone of both horizontal and vertical thin sections and at each point an area of 5 μm^2 to a depth of 5 μm was analysed and all the elements available were listed. EDX analysers have variable detection limitations. In this case, some elements, typically oxygen, carbon and hydrogen could not be detected. However, silica, SiO_2, was one of the major elements that were detected, as shown in Figs. 6 and 7 and quantified. Hence, a comparison between the plain mortar and 20% SF mortar was possible.

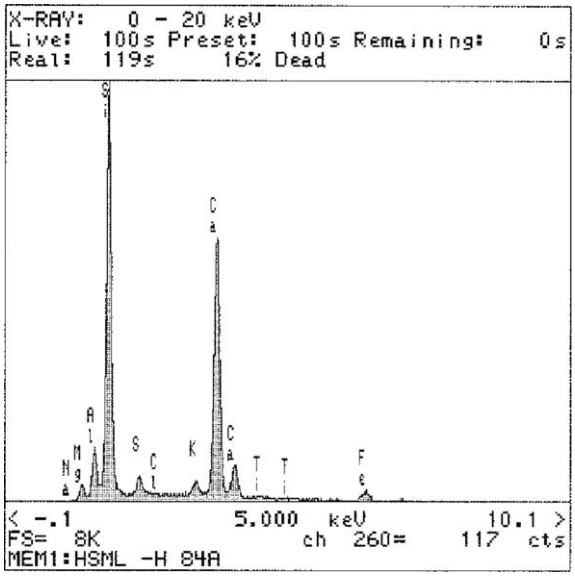

Fig. 6. EDX analysis of Point-84A in the interface.

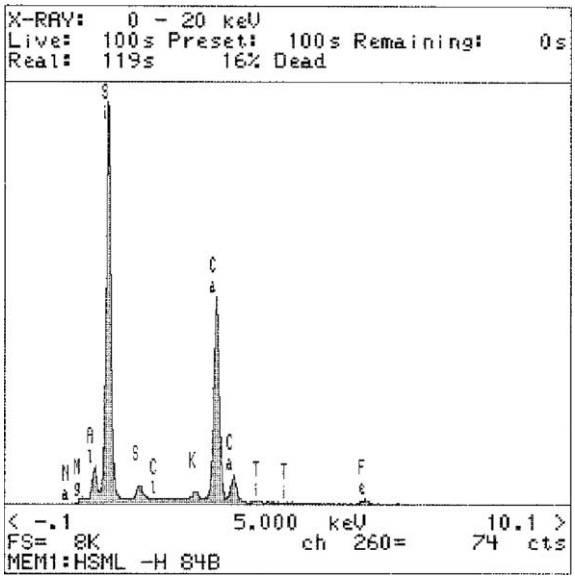

Fig. 7. EDX analysis of Point-84B in the interface.

2.4. Experimental method for aggregate push-out experiments

In the interfacial area, researchers [11,13,20–22] have used different techniques and different test methods over the years, as there is no universally accepted and standardised test method, by which the interfacial bond strength can be obtained. Many difficulties are faced in the study of interface in actual concrete samples, such as how to apply the load to the interfacial area. This has led the researchers [8,9,23–31] to utilise the test samples, which contain an artificially prepared (mostly cored) single aggregate. This allows one to apply the load directly to the aggregate, and to locate the aggregate in any desired location within the concrete body.

For each aggregate diameter and aggregate type, five specimens were tested for aggregate push-out, which makes approximately 120 test specimens in total. Aggregate push-out tests were conducted by using the general set-up shown in Fig. 8. The load was applied only to the cylindrical aggregate part of the specimen, while the mortar matrix was fully supported except for a 0.5 mm rim around the cylindrical aggregate to allow the aggregate to be pushed through the circular hole without any disturbances. Interfacial bond strength, τ (MPa) was obtained by dividing the maximum load, P_{max} by the nominal shear area which is given by the product of the circumference of the cylindrical aggregate and the depth, ($\tau = P_{max}/2\pi rL$) where L is the constant length of the cylindrical aggregate as 20 mm and r is the radius in mm.

3. Results and discussion

3.1. Thickness of interface

Fig. 9 shows the average results of the interfacial thickness study. The comparison of the interfacial zone thickness results on the basis of the mortar types used show that there is a noticeable difference between the plain mortar and 20% SF mortar specimens. Irrespective of the aggregate types used, 20% SF mortar specimens provided the lowest thickness values. It can therefore, be said that the higher the mortar strength, the thinner the interfacial thickness regardless of the aggregate types. This can, in fact, be attributed to the presence of the SF and the use of SP. While the first provides a denser interface by acting as a filler and providing secondary hydration products, the second helps towards deflocculation of the cement and silica fume particles, and reduction in the water content of the mix, as well as providing extra consistency.

When the interfacial zone thickness results are compared on the basis of different aggregate types located in the centre of the specimens, one can see that limestone aggregates provided noticeably thinner interfacial zone than that of granite and sandstone aggregates irrespective of the mortar types used. This is probably related to the chemical structure of the aggregates. Whilst both sandstone and granite are essentially quartz (SiO_2) based, limestone is primarily calcium carbonate ($CaCO_3$), which could react with the hydration products leading to a thinner interfacial zone. While the contribution of SF and SP to the interface is clear and significant on the basis of the relative interfacial thickness, more research is needed to establish a relationship between the interfacial thickness and the aggregate types.

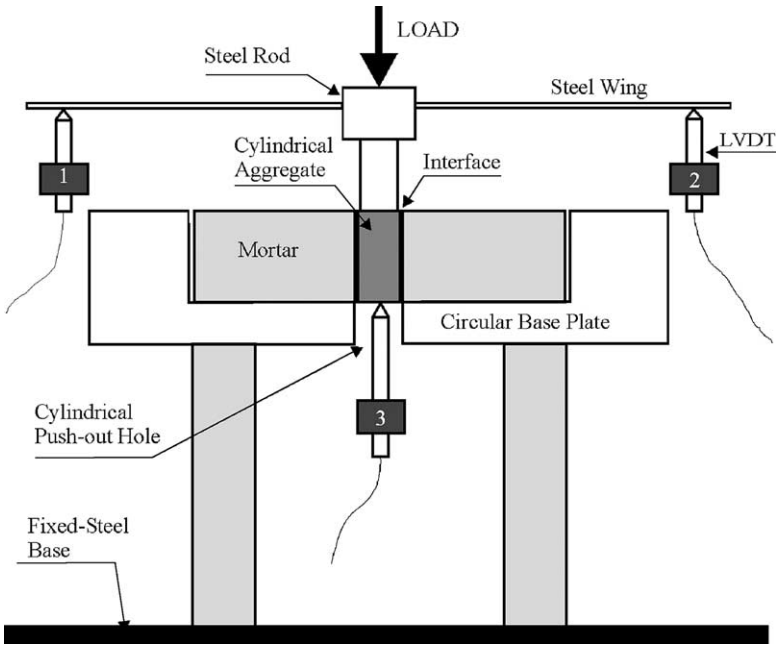

Fig. 8. General view of the aggregate push-out test set-up.

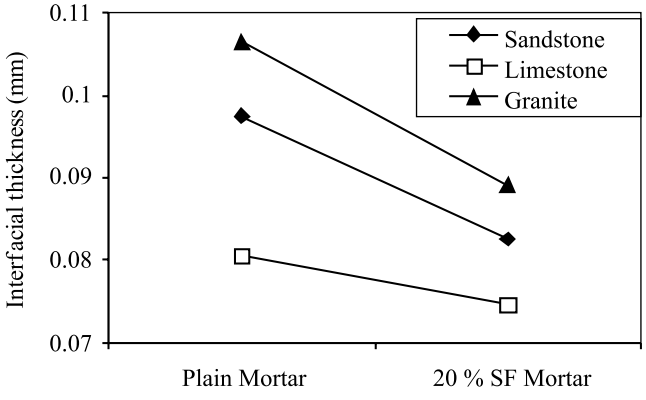

Fig. 9. Interfacial thickness at cylindrical aggregate/mortar interface.

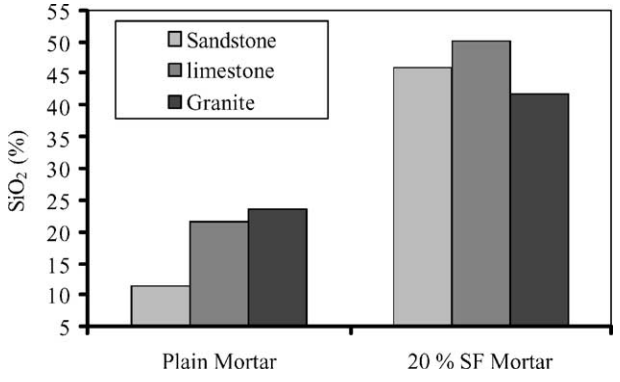

Fig. 10. Deposition of silica (SiO_2) in the aggregate/mortar interface.

3.2. Silica (SiO_2) content in the interface

To reveal the contribution of SF to the SiO_2 content at the interface, a series of chemical investigations were undertaken on the interfacial zone between different types of cylindrical aggregates and different types of mortar matrices by using EDX analyzer. Fig. 10 illustrates the variation of silica content in the interface versus mortar types on the basis of different aggregate types used. One can observe in this figure that the amount of SiO_2 in the interface increases considerably as the 20% SF was replaced with cement in mix, regardless of the aggregate types used.

It is interesting to note that in the case of both sandstone and limestone aggregates the increase of SiO_2 deposition in the interface is far more than the percentage of the SF added to the mix. In either case the increase is more than 100%. For example, sandstone aggregates with plain mortar provided about 10% SiO_2, while the same type of aggregate with 20% SF mortar provided about 45% SiO_2 content. This increase in fact is in agreement with the relative interfacial thickness results where SF mortar provided the thinner interface. This clearly indicates how the interfacial zone was densified by the inclusion of SF and SP.

3.3. Aggregate push-out test results

Interfacial bond strength, τ results from the aggregate push-out tests are presented in Fig. 11(a)–(c) on a logarithmic scale. A comparison between sandstone,

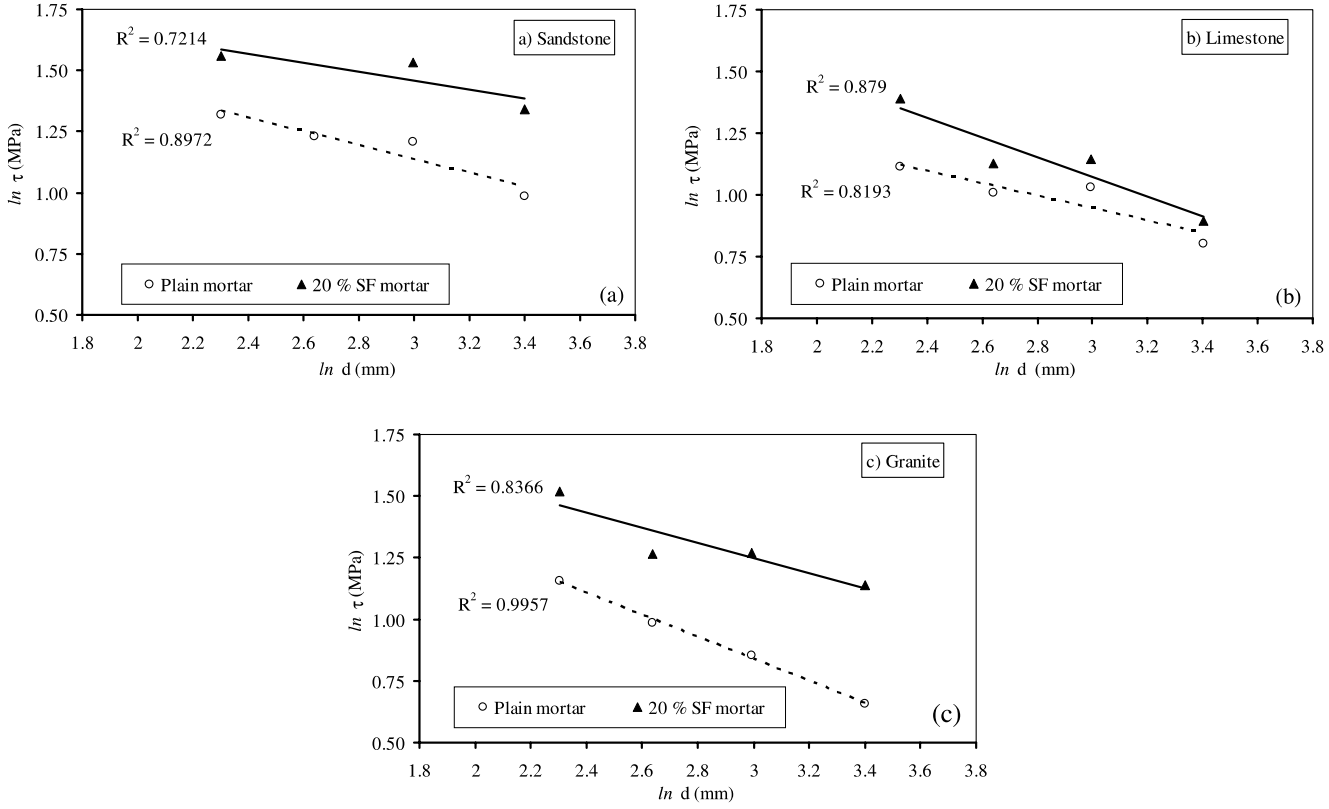

Fig. 11. Variation of bond strength with aggregate diameter for varying mortar and aggregate combinations.

limestone and granite is made for τ results on the basis of mortar types in Fig. 11(a)–(c), respectively, where one can observe that 20% SF mortar specimens provide significantly higher interfacial bond strength values than that of plain cement mortar, regardless of the aggregate diameters and types used. This finding is in fact in agreement with both interfacial thickness results and the quantity of SiO_2 in the interface, i.e., the higher the SiO_2 amount in the interface, the thinner (denser) the interface and the stronger the interfacial bond strength between the cylindrical aggregates and the mortar matrix. As the types of the aggregate are taken into account, it is clear that the sandstone aggregates provided the highest interfacial bond strength, followed by the granite and then limestone aggregates, regardless of the diameters of the aggregate and the mortar types used. This could probably be related to the coarse texture of sandstone, which provides extra strong mechanical interlocking between the mortar matrix and the aggregate.

It is also shown in Fig. 11(a)–(c) that the results of interfacial bond strength obtained by means of aggregate push-out tests present a distinct size effect that as the size of the aggregate reduces the interfacial bond strength increases significantly irrespective of both mortar and aggregate types. It is believed that the size effect observed is a statistical kind and it can be described by a power law relationship of the Weibull type as follows:

Table 5
Experimental regression coefficients A and n

Aggregate type	Plain mortar		20% SF mortar	
	A	n	A	n
Sandstone	7.34	0.28	7.42	0.18
Limestone	5.49	0.25	9.74	0.40
Granite	8.86	0.45	8.74	0.31

$$\tau = A * d^{-n} \quad (1)$$

where d (mm) is the diameter of the aggregate and A and n are the regression coefficients, which are given in Table 5.

4. Conclusions

1. Generally, 20% silica fume replacement with cement and addition of super plasticizer to the mortar produced a thinner interfacial zone than the plain cement mortar. This stems from the fact that SF densifies the microstructure by acting as a filler as well as providing a secondary hydration products, while SP provides deflocculation of the cement and silica fume particles, as well as extra flow capability to the mix so that better packing would be possible.
2. 20% silica fume replacement of cement increased the amount of SiO_2 content significantly in the interfacial

zone between cylindrical aggregates and mortar matrices.

3. 20% silica fume replacement of cement provided the higher interfacial bond strength, τ than that of plain cement mortar regardless of aggregate diameter and types. The relationship between the τ and the interfacial thickness and the SiO_2 content is significant, i.e. the higher the strength of the matrix (as a result of the SF replacement), the thinner the relative thickness of the interface, the higher the deposition of the SiO_2 content in the interface and the higher the τ.
4. There is a distinct statistical size effect between the bond strength and the aggregate diameter irrespective of aggregate and mortar types used, i.e., as the aggregate size reduces the bond strength increases.

Acknowledgements

The author would like to thank to Prof. B.L. Karihaloo and Prof. B.I.G. Barr (Department of Civil Engineering, Cardiff University, UK) for their help and valuable remarks on this paper.

References

[1] Karihaloo BL. In: Fracture mechanics structural concrete. Essex: Longman; 1995. p. 330.
[2] Caliskan S, Karihaloo BL, Barr BIG. Study of rock–mortar interfaces. Proceedings of the Concrete Communication Conference 2000, University of Birmingham 2000;29–30(June):59–68.
[3] Neville AM. In: Properties of Concrete. Forth ed. London: Longman; 1995. p. 844.
[4] Bentz DP, Stutzman PE, Garboczi EJ. Experimental and simulation studies of the interfacial zone in concrete. Cement Concrete Res 1992-A;22:891–902.
[5] Buyukozturk O, Lee KM. Fracture of mortar–mortar interfaces in concrete composites. In: Maso JC, editor. Interfaces in Cementitious Composites. London; 1992-A. p. 139–48.
[6] Buyukozturk O, Lee KM. Interface fracture mechanics of concrete composites. In: Bazant ZP, editor. Proceedings of the First Conference on Fracture Mechanics of Concrete structures (FraMCoS1). Colorado; 1992-B. p. 163–68.
[7] Bentz DP, Hwang JTG, Hagwood C, Garboczi EJ, Snyder KA, Buenfeld N, Scriviner KL. Interfacial zone percolation in concrete: effects of interfacial zone thickness and aggregate shape. In: Diamond S, editor. Microstructure of Cement-Based Systems/Bonding and Interfaces in Cementitious Materials. Pittsburg; 1995. p. 437–442.
[8] Lee KM, Buyukozturk O, Oumera A. Fracture analysis of mortar-aggregate interfaces in concrete. J Eng Mech 1992;118(10):2031–47.
[9] Tasong WA, Lynsdale CJ, Cripps JC. Aggregate–cement paste interface. II. Influence of aggregate physical properties. Cement Concrete Res 1998;28(10):1453–65.
[10] Mindess S. The application of fracture mechanics to cement and concrete: a historical review. In: Wittman FH, editor. Fracture Mechanics of Concrete. Amsterdam: Elsevier Science Publishers B.V.; 1983. p. 1–30.
[11] van Mier JGM. In: Fracture Processes of Concrete: Assessment of Material Parameters for Fracture Models. London: CRC Press; 1997. p. 448.
[12] Bentz DP, Garboczi EJ. Simulation studies of the effects of mineral admixtures on the cement paste–aggregate interfacial zone. ACI Mater J 1991;88(5):518–29.
[13] Tschegg EK, Rotter HM, Roelfstra PE, Bourgund U, Jussel P. Fracture mechanical behaviour of aggregate–cement matrix interfaces. J Mater Civil Eng 1995;7(4):199–203.
[14] Rachel JD, Kumar PM. Chemical and physical effects of silica fume on the mechanical behavior of concrete. ACI Mater J 1989;86(6):609–14.
[15] Zhang M, Gjorv OE. Microstructure of the interfacial zone between lightweight aggregate and cement paste. Cement Concrete Res 1990;20:610–8.
[16] British Standard Institution BS 1881:116:1983. Method for Determination of Compressive Strength of Concrete Cubes, London.
[17] British Standard Institution BS 1881:117:1983. Method for Determination of Tensile Splitting Strength, London.
[18] British Standard Institution BS 1881:121:1983. Method for Determination Static Modulus of Elasticity in Compression, London.
[19] American National Standard. ASTM C 170-50, (Reapproved 1981). Standard Test Method for Compressive Strength of Natural Building Stone.
[20] Alexander MG. Two experimental techniques for studying the effects of the interfacial zone between cement paste and rock. Cement Concrete Res 1993;23:567–75.
[21] Monteiro PJM, Andrade WP. Analysis of the rock–cement paste bond using probabilistic treatment of brittle strength. Cement Concrete Res 1987;17:919–26.
[22] Tasong WA, Lynsdale CJ, Cripps JC. Aggregate–cement paste interface Part I. Influence of aggregate geochemistry. Cement Concrete Res 1999;29:1019–25.
[23] Mitsui K, Li Z, Lange DA, Shah SPA. A study of properties of the paste–aggregate interface. In: Maso JC, editor. Interfaces in Cementitius Composites. London: E&FN Spon; 1992. p. 119–28.
[24] Mitsui K, Li Z, Lange DA, Shah SP. Relationship between microstructure and mechanical properties of the paste–aggregate interface. ACI Mater J 1994;91(1):30–9.
[25] Vervuurt AHJM. Interface Fracture in Concrete. PhD Thesis, Delft University, Netherlands, 1997. p. 165.
[26] Mohamed AR, Hansen W. Micromechanical modelling of crack–aggregate interaction in concrete materials. Cement Concrete Compos 1999;21:349–59.
[27] Caliskan S, Karihaloo BL, Barr BIG. Study of rock mortar interfaces. Part I: Surface roughness of rock aggregates and microstructural characteristics of interface. Mag Concrete Res, 2002 (in press).
[28] Caliskan S, Karihaloo BL, Barr BIG. Study of rock mortar interfaces. Part II: Strength of interface. Mag Concrete Res, 2002 (in press).
[29] Tasdemir C, Akyuz S, Tasdemir MA. Betonda Agrega-Cimento Hamuru Temas Yuzeyinin Mekanik Davranistaki Islevi, IX, Ulusal Mekanik Kongresi, Urgup, Eylul 1995. p. 674–683 (in Turkish).
[30] Saito M, Kawamura M. Resistance of the cement–aggregate interfacial zone to the propagation of cracks. Cement Concrete Res 1986;16:653–61.
[31] Jiang L. The interfacial zone and bond strength between aggregates and cement pastes incorporating high volumes of fly ash. Cement Concrete Compos 1999;21:313–6.